Volume 1 | Number 1 | Jan 2013 | Pages 1–100

ChemComm

Chemical Communications
www.rsc.org/chemcomm

ROYAL SOCIETY OF CHEMISTRY

ROYAL SOCIETY OF CHEMISTRY

www.rsc.org/chemcomm

ChemComm

Communication

Semimetal bismuth element as a direct plasmonic photocatalyst

Fan Dong[a]*, Ting Xiong[a], Yanjuan Sun[a]*, Zaiwang Zhao[a], Ying Zhou[b], Xin Feng[a], Zhongbiao Wu[c]

The bismuth element synthesized by a facile chemical solution method exhibited admirable and stable photocatalytic activity towards removal of NO under 280nm light irradiation due to the surface plasmon resonance mediated direct photocatalysis, and most strikingly, showed a catalytic "memory" capability following illumination.

Photocatalysis technology has received intensive attention as a potential solution to urgent global issues of energy shortage and environmental pollution.[1-3] Conventional photocatalysts (TiO_2, Bi_2WO_6 et al) are semiconductors with a band gap structure.[4-5] Light absorption and the consequent photoexcitation of electron-hole pairs take place when the energy of the incident photons matches the band gap, and then the excited electrons and holes migrate to the surface to initiate chemical reactions. In the past decade, the surface plasmon resonance (SPR) of noble metal (Au and Ag) nanoparticles has been shown to improve the photocatalysis efficiency of the substrate semiconductors.[6] The excitation of surface plasmon resonance is employed to transfer photon energy to nearby indispensible semiconductor/molecular photocatalysts. Recently, isolated noble metal photocatalysts without relying on other semiconductor/molecular photocatalysts were considered as new direct plasmonic photocatalysts.[7] These noble metal nanoparticles can act as the light absorber and the catalytically active site simultaneously. For example, Chen et al. reported the visible-light-driven oxidation of organic contaminants in air with gold nanoparticle catalysts on oxide supports.[8] Linic's group found the visible-light-enhanced catalytic oxidation reactions on plasmonic silver.[9] Very recently, Guo et al. fabricated copper nanoparticles on graphene support for plasmonic photocatalytic coupling of nitroaromatics.[10] These direct metal based plamonic photocatalysts open up new avenues towards discovering novel photocatalytic materials.

Bismuth, a typical semimetal material, has attracted great interests with a set of unique properties, such as very small effective masses, large mean free path, long Fermi wavelength, high carrier motilies, and very small band overlap energy. Moreover, nano-confinement effects, observed in Bi element, allows a semimetal-to-semiconductor transition at diameters of a few tens of nanometers.[11] Similar to Au and Ag, Bi has been found to exhibit plasmonic properties.[12] Collective excitation of free electrons in semimetal Bi gives rise to the SPR phenomenon, which results in a strong resonant optical absorption as well as near-field and scattering enhancements. This strong SPR-mediated effect with semimetal Bi has been exploited in many applications, including sensors, fluorescence and surface-enhanced spectroscopy.[13] The Bi element has also been applied in photocatalysis based on its photosensitization or narrow energy band.[14] However, to our knowledge, studies concerning the mechanism and application of Bi nanostructures in photocatalysis utilizing the surface plasmon resonance have never been reported.

Herein, we synthesized Bi nanoparticles by a facile chemical solution method. The Bi nanoparticles are found to display SPR property in near ultra-violet and visible range. Moreover, the as-prepared Bi exhibited admirable and stable photocatalytic activity towards removal of NO under 280nm light irradiation, resulting from direct photocatalysis mediated by the SPR of Bi element, and showed an impressive catalytic "memory" capability.
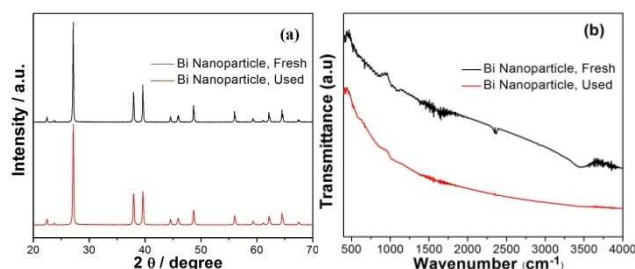

Fig. 1 XRD patterns (a) and FT-IR (b) of Bi nanoparticles for fresh and used samples.

The detailed procedure for the experiments was described in ESI. The XRD of Bi nanoparticles (Fresh) in Fig. 1a shows that all the diffraction peaks can be exactly indexed to the rhombohedral phase of elemental Bi (JCPDS card no. 05-0519) without any other impurity phases. In addition, except the stretching vibration absorption of hydroxyl groups (3445 cm^{-1}), no other absorption can be observed in FT-IR spectra (Fresh). However, Bi-O bond was detected by XPS. After sputtering for 15nm of the Bi nanoparticles surface, the Bi-O bond was still detected due to the fact that Bi element can be easily oxidized by O_2 in air. These phenomena imply that a thin amorphous bismuth oxide layer exists on the surface (Fig. S1 (ESI†)).

The SEM image in Fig. 2a shows the overall morphology of Bi sample. A large amount of Bi nanoparticles can be observed. Fig. 2b further demonstrates that the Bi sample with particle size around 100-200 nm. Fig. 2c exhibits the HRTEM image of an individual Bi nanoparticle. The spacing of 0.223 nm corresponds to the (110) plane of rhombohedral Bi. Also, the boundary of the crystal face can be observed in Fig. 2c, further demonstrating the surface amorphous layer is thin. The SAED in Figure 2d displays an array of clear and regular diffraction spots, indicating that the

Bi particle is well-defined single crystalline. The specific surface area of Bi sample is determined to be 1.2 m^2/g obtained from nitrogen adsorption–desorption isotherms (Fig. S2 (ESI†)).
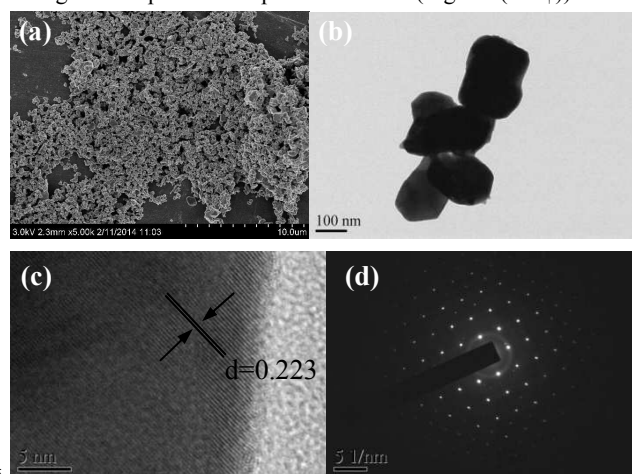

Fig. 2 SEM (a) and TEM images (b and c) of Bi sample, SAED of an individual Bi particle (d).

Toudert et al reported that semimetal Bi displays SPR property in near ultra-violet and visible range if the particle size of Bi is larger than 100 nm.[12] From Fig. S3 (ESI†), a strong and broad absorption peak at ca. 280 nm in the ultraviolet can be observed, which is the dominant plasmon resonance peak of Bi nanoparticles. This plasmon resonance peak has previously been observed in bismuth nanoparticles.[15-16] In the visible light region, the spectra are featured by a broad plasmon absorption band. Light scattering effect becomes obvious because of the large size, which widens the plasmon absorption peak. For Bi (III) species, a main absorption peak appeared at around 316 nm, which is different from literature.[17] In addition, Bi nanoparticles exhibited photoelectrochemical performance under both UV-visible and visible (λ > 420 nm) light illumination (Fig. S4, ESI†), consistent with the light absorption range in UV-vis DRS (Fig. S3, ESI†).

The photocatalytic activity of Bi nanoparticles was evaluated towards removal of NO under light irradiation. Fig. 3a shows the variation of NO concentration (C/C_0 %) with irradiation time over Bi nanoparticles. Here, C_0 and C are the concentration of NO at time zero and t, respectively. The removal ratio of NO is 9.2 % without photocatalyst under 280 nm light irradiation due to the direct UV induced transformation of NO, while a removal ratio of 46.0 % can be observed when using Bi nanoparticles as photocatalyst. It is surprising to find that the Bi nanoparticles show negligible photocatalytic activity under 360 and 420nm light irradiation, which indicates that the absorption at these wavelengths is inefficient to initiate photocatalysis. More interestingly, we can find that the catalyst still remains active for an extended period of time when the photoexcitation is turned off. This phenomenon is defined as catalytic "memory" capability.

The reaction intermediate of NO$_2$ during photocatalytic oxidation of NO is monitored on-line as shown in Fig. S5a (ESI†). The fraction of NO$_2$ generated without photocatalyst (77.2 %) is higher than that with Bi nanoparticles (30.2 %). The diffusion of reaction intermediate over Bi nanoparticles promotes the oxidation of intermediate NO$_2$ to final NO$_3^-$. As shown in Fig. 3b, the Bi sample still maintains stable photocatalytic activity towards removal of NO without any obvious deactivation after five repetitive cycles. Meantime, the Bi nanoparticles exhibit durable photocatalytic activity (Fig. S5b (ESI†)) for more than 5 h irradiation. In addition, we can find the XRD and FT-IR spectra of Bi nanoparticle after long time irradiation (Used sample shown in Fig. 1) are almost identical to the fresh sample. These facts suggest that the as-prepared Bi nanoparticles have excellent phase stability and performance stability.
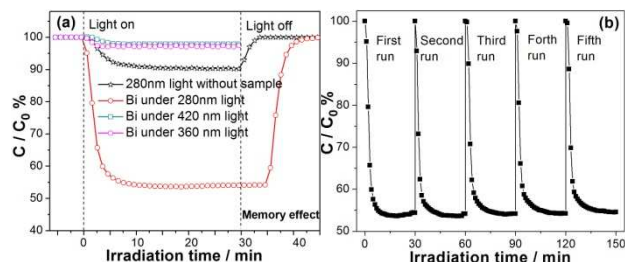

Fig. 3 Photocatalytic removal of NO in air over Bi nanoparticles (a) and repeated photocatalytic activity under 280nm light (b).

To investigate the reactive species and mechanism accounting for the photocatalytic oxidation of NO, we measured the DMPO spin-trapping ESR spectra of Bi nanoparticles in aqueous dispersion for DMPO-•OH (Figure 4a) and in methanol dispersion for DMPO-•O$_2^-$ (Figure 4b). Under light illumination (280nm), the characteristic peaks of DMPO-•OH and DMPO-•O$_2^-$ can be observed, indicating the production of •OH and •O$_2^-$ on Bi nanoparticles. To determine the fate of •OH and •O$_2^-$ generated during the irradiation period, we turned off the illumination instantly and monitored the variation of ESR signals with time in the dark. As displayed in Fig. 4a and 4b, the signals of DMPO-•OH and DMPO-•O$_2^-$ could still be observed even after the illumination was switched off. After staying in the dark for 10 min, the ESR intensity of the signals of Bi remained almost un-changed. This fact agrees with the extended photocatalytic activity of Bi after turning off the light (Fig. 3a).
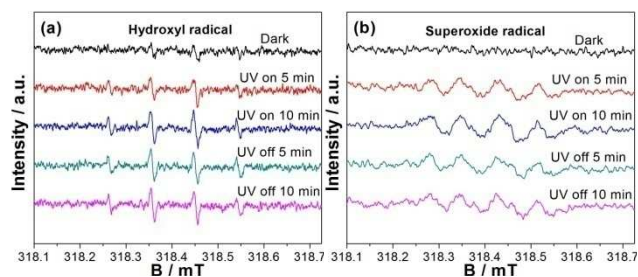

Fig. 4 DMPO spin-trapping ESR spectra of Bi nanoparticles in aqueous dispersion for DMPO-•OH (a) and in methanol dispersion for DMPO-•O$_2^-$ (b).

Following light absorption and SPR excitation in Bi nanoparticles, the plasmon decay will takes place through three mechanisms,[7] (1) elastic radiative reemission of photons, where adsorbed molecules can gain energy through the absorption of photons from intense, reradiated photon fluxes from the plasmonic nanostructure, (2) nonradiative Landau damping, where photon energy is converted to single e$^-$/h$^+$ pair excitations. The excited primary electrons interact with other electrons through Coulombic inelastic scattering to produce many electrons, and (3) the interaction of excited surface plasmons with

adsorbates, inducing direct electron injection into the adsorbates. Bi nanoparticles showed admirable photocatalytic activity under 280nm light irradiation, and active species ($\cdot$OH and $\cdot O_2^-$) were detected. Thus, it is supposed that the plasmon decay at 280nm takes place though (2) and (3), and may including (1) (NO can be removed by absorbing intense, reradiated photon fluxes from Bi nanostructure due to the high energy of light at 280nm can be further enhanced though SPR). However, Bi nanoparticles showed negligible activity when the wavelength exceeds 360nm. The photocurrent-voltage results of Bi nanoparticles imply that electrons and holes are generated under visible light illumination. Thus, the plasmon decay in visible light region can take place though (2) and (3). The poor photocatalytic activity may result from the fact that the potential of electrons or holes are not negative or positive enough to induce the production of $\cdot O_2^-$ and $\cdot$OH as shown in Fig. S6 (ESI†). Zhu et al. have tuned the reduction power of supported gold nanoparticle photocatalysts for selective reductions by manipulating wavelength of visible light irradiation.[18] The plasmon decay may also be through (1), while the photon absorption is insufficient to break the N-O bond. These analysis also suggest that the photoabsorption and photocatalytic activity of the sample are not caused by the surface bismuth oxide layer because NO can be removed by bismuth oxide under visible light.[19] The corresponding action spectrum of Bi nanoparticles is shown in Fig. S7 (ESI†). In addition, the catalytic "memory" capability may stem from the long lived and stable reactive species on the surface following illumination. Similar phenomenon has been found in Se element.[20] When the light is turned off, the reactive species are considered not to disappear instantly but to initiate chemical reaction afterwards. Consequently, Bi nanoparticles exhibited an interesting catalytic "memory" effect. The relating reactions are shown in Eqs. (a)-(f).

$$BlackBi + h\nu \rightarrow h^+(Bi) + e^-(Bi) \quad (a), \qquad H_2O + h^+ \rightarrow \cdot OH + H^+ \quad (b),$$
$$O_{2(ads)} + e^- \rightarrow \cdot O_2^- \quad (c), \qquad NO + 2\cdot OH \rightarrow NO_2 + H_2O \quad (d),$$
$$NO_2 + \cdot OH \rightarrow NO_3^- + H^+ \quad (e), \qquad NO + \cdot O_2^- \rightarrow NO_3^- \quad (f),$$
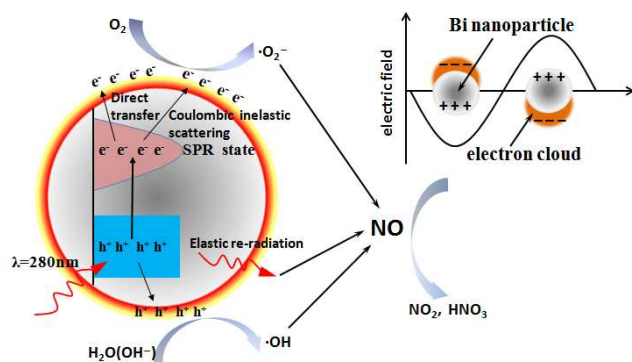

Fig. 5 Schematic diagram of the plasmonic photocatalysis mechanism of Bi nanoparticles.

In summary, we synthesized bismuth nanoparticles by a facile chemical solution method and applied it for removal of NO in air utilizing its direct plasmonic photocatalysis. The semimetal Bi nanoparticles exhibited admirable and stable photocatalytic activity under 280nm light irradiation. Meantime, catalytic "memory" of Bi element is observed. The photocatalytic activity and the catalytic "memory" of Bi nanoparticles can be ascribed to the UV-mediated surface plasmon resonance and the long lived active species, respectively. The discovery of Bi element as a direct plasmonic photocatalyst is of great significance as it is expected to shed new light on the understanding and application of plasmonic photocatalysis mediated by non-noble metals.

Notes and references

a Chongqing Key Laboratory of Catalysis and Functional Organic Molecules, College of Environmental and Biological Engineering, Chongqing Technology and Business University, Chongqing, 400067, China.
b School of Materials Science and Engineering, Southwest Petroleum University, Chengdu, 610500, China.
c Department of Environmental Engineering, Zhejiang University, Hangzhou 310027, PR China.
∗ To whom correspondence should be addressed.
E-mail: dfctbu@126.com (Fan Dong), syhsyj@163.com(Yanjuan Sun). Tel.: +86-23-62769785-605; Fax: +86-23-62769785-605.
†Electronic supplementary information (ESI) available: Experimental details, characterization, and Fig. S1 to S7. See DOI: 10.1039/b000000x/

1 (a) A. Fujishima and K. Honda, *Nature*, 1972, **238**, 37; (b) P. V. Kamat, *Chem. Rev.*, 1993, **93**, 267.
2 (a) A. Hagfeldt and M. Gratzel, *Chem. Rev.*, 1995, **95**, 49; (b) M. R. Hoffmann, S. T. Martin, W. Y. Choi and D. W. Bahnemann, *Chem. Rev.*, 1995, **95**, 69.
3 K. Awazu, M. Fujimaki, C. Rockstuhl, J. Tominaga, H. Murakami, Y. Ohki, N. Yoshida and T. Watanabe, *J. Am. Chem. Soc.*, 2008, **130**, 1676.
4 G. Liu, L. Z. Wang, H. G. Yang, H. M. Cheng and G. Q. Lu, *J. Mater. Chem.*, 2010, **20**, 831.
5 L. Zhang and Y. Zhu, *Catal. Sci. Technol.,* 2012, **2**, 694.
6 (a) P. Wang, B. B. Huang, Y. Dai and M. H. Whangbo, *Phys. Chem. Chem. Phys.*, 2012, **14**, 9813; (b) X. M. Zhou, G. Liu, J. G. Yu and W. H. Fan, *J. Mater. Chem.*, 2012, **22**, 21337; (c) S. Linic, P. Christopher and D. B. Ingram, *Nature. Mater.*, 2011, **10**, 911; (d) C. Clavero, *Nat. Photonics.*, 2014, **8**, 95.
7 (a) M. J. Kale, T. Avanesian and P. Christopher, *ACS Catal.*, 2014, **4**, 116; (b) P. Christopher, H. L. Xin, A. Marimuthu and S. Linic, *Nat. Mater.*, 2012, **11**, 1044; (c) S. C. Warren and E. Thimsen, *Energy Environ. Sci.*, 2012, **5**, 5133.
8 X. Chen, H. Y. Zhu, J. C. Zhao, Z. F. Zheng and X. P. Gao, *Angew. Chem. Int. Ed.*, 2008, **47**, 5353.
9 P. Christopher, H.L. Xin and S. Linic, *Nat. Chem.,* 2011, **3**, 467.
10 X. N. Guo, C. H. Hao, G. Q. Jin, H. Y. Zhu and X. Y. Guo, *Angew. Chem. Int. Ed.*, 2014, **53**, 1.
11 (a) E. Gerlach, P. Grosse, M. Rautenberg and W. Senske, *Phys. Status Solidi B.*, 1976, **75**, 553; (b) F. Y. Yang, K. Liu, C. L. Chien and P. C. Searson, *Phys. Rev. Lett.*,1999, **82**, 3328.
12 (a) J. Toudert, R. Serna, and M. J. Castro, *J. Phys. Chem. C.*, 2012, **116**, 20530. (b) J. M. McMahon, G. C. Schatz and S. K. Gray, *Chem. Chem. Phys.*, 2013, **15**, 5415.
13 R. Tediosi, N. P. Armitage, E. Giannini and D. van der Marel, *Phys.Rev. Lett.*, 2007, **99**, 016406.
14 (a) D. Ma, J. Z. Zhao, Y. Zhao, X. L. Hao and Y. Lu, *Chem. Eng. J.*, 2012, **209**, 273; (b) F. Qin, R. M. Wang, G. F. Li, F. Tian, H. P. Zhao and R. Chen, *Catal. Commun.*, 2013, **42**, 14; (c) Z. Wang, C. L. Jiang, R.Huang, H. Peng and X. D. Tang, J. *Phys. Chem. C.*, 2014, **118**, 1155.
15 G. Maritza and H. Arnim, *J. Phys. Chem.*, 1996, **100**, 7656.
16 D. Ma, J. Z. Zhao, Y. Zhao, X. L. Hao, L. Z. Li, L. Zhang, Y. Lu and C. Z. Yu, *Colloids and Surfaces A: Physi.*, 2012, **395**, 276.
17 D. Velasco-Arias, I. Zumeta-Dubé, D. Díaz, P. Santiago-Jacinto, V.-F. Ruiz-Ruiz, S.-E. Castillo-Blum and L. Rendón, *J. Phys. Chem. C.*, 2012, **116**, 14717.
18 X. Ke, S. Sarina, J. Zhao, X. Zhang, J. Chang and H. Zhu, *Chem. Commun.*, 2012, **48**, 3509.
19 Z. H. Ai, Y. Huang, S. C. Lee and L. Z. Zhang, *J. Alloy. Compd.*, 2011, **509**, 2044.
20 Y. D. Chiou and Y. J. Hsu, *Appl. Catal. B.,* 2011, **105**, 211.